Magnesium Technology 2016
Edited by: Alok Singh, Kiran Solanki, Michele V. Manuel, and Neale R. Neelameggham
TMS (The Minerals, Metals & Materials Society), 2016

Mechanical Response of a Gravity Cast Mg-9Al-1Zn-0.2Sc Alloy at Strain Rates from 10^{-4} to 10^{3} /s

R.B. Blessington[1], A.D. Brown[1], A. Lock[1], J.P. Escobedo[1], P.J. Hazell[1], D. East[2], M.Z. Quadir[3]
[1]School of Engineering and Information Technology, The University of New South Wales, Canberra, ACT, Australia
[2]CSIRO Manufacturing Flagship, Clayton, VIC, Australia
[3] Mark Wainright Analytical Centre, Electron Microscope Unit, UNSW Australia, NSW, Australia

Keywords: magnesium, scandium, Split Hopkinson Pressure Bar, microstructure, strain rate

Abstract

A magnesium alloy of nominal composition Mg-9Al-1Zn-0.2Sc was formed into plates by die casting and underwent annealing and T4 condition heat treatments to investigate the mechanical response of varying microstructures at strain rates from 10^{-4}-10^{3}/s in tension and compression. Full microstructural characterization was performed using optical microscopy, electron backscatter diffraction and energy dispersive x-ray spectroscopy. Quasi-static and dynamic testing was performed using a universal testing machine and a Split Hopkinson Pressure Bar in conjunction with digital image correlation for strain field mapping. Characterization and mechanical testing indicates that the T4 condition has the highest overall strength due to small equiaxed grains, a decrease in the size of β-$Mg_{17}Al_{12}$ phase at the grain boundaries, and an increase in the size of scandium intermetallics. Testing indicates an increase in strain hardening for dynamic compression and strain rate dependence in tension; failing suddenly due to casting defects dominating the fracture mechanics.

Introduction

Due to the need for lightweight metals in the aerospace and automotive industries, the interest in magnesium alloy systems has received renewed attention [1]. However, the degradation of mechanical properties at elevated temperatures, as low as 373K, limits their use in many applications [14].The addition of rare earth metals to magnesium alloys, specifically Scandium, has been shown to improve yield strength at both room and elevated temperatures during quasi-static testing [2-4, 15]. The strengthening effects have been concluded to be a result of limiting the formation of β-$Mg_{17}Al_{12}$ phase due to the formation of the Mg_5Al_4Sc intermetallic compound at grain boundaries, which is effective at inhibiting dislocation motion at room and elevated temperatures [2].

The effects of scandium on the dynamic properties of magnesium alloys has yet to be explored significantly, as well as the effects of heat treatments have on the mechanical properties of scandium containing magnesium alloys [2]. The primary aim of this study is to investigate the effects of scandium on the mechanical properties of magnesium alloys for quasi-static and dynamic loading conditions for multiple thermal processing conditions.

Experimental Methods

A magnesium alloy of nominal percent weight composition Mg-9Al-1Zn-0.2Scwas cast as a plate in a tool steel mold was received from the Commonwealth Scientific and Industrial Research Organization (CSIRO).Two further heat treatments were performed on the received material in an inert CO_2 atmosphere to investigate effects on the mechanical properties due to grain size effects and the growth of second phases and intermetallics at the grain boundaries (GBs). The heat treatments investigated were classified as: fully annealed (723K for 24h then furnace cooled) and the T4 condition (648K for 3h, 688 K for 18h, then quenched in water) [2,5].

The characterization of the material has been undertaken using optical microscopy, electron backscatter diffraction (EBSD) and energy dispersive x-ray spectroscopy (EDS). The EDS was performed in parallel with the EBSD data collection, which required the specimen to be at a tilt angle of 70°, theoretically making the data slightly less quantitatively accurate than standard EDS procedure carried out at 0° tilt. Analysis of the EBSD data of for all three material conditions revealed a distinct lack of crystallographic texture as shown by the inverse pole figures (IPFs) in Fig. 1a through 1c; which was expected due to the cast nature of the material. The average area grain sizes for each microstructure were as follows: 380μm for as-cast, 319μm for annealed, and 127μm for T4. The grain shapes for all material conditions were fairly equiaxed, with the T4 condition having a slightly dendritic grain structure. Data obtained from EDS clearly indicates significant differences in the composition of phases at the GBs within the annealed and T4 material conditions, as indicated by Fig. 1d through 1g. The annealed material condition contains greater amounts of the β-$Mg_{17}Al_{12}$ phase at the GBs than compared to the T4 condition. Additionally, the size of the strengthening Mg_5Al_4Sc intermetallic compound particles greatly increased in size from the annealed to T4 material conditions. This coupled with their respective β-phase amounts and differences in grain sizes, should lead to an increase in the mechanical properties in the T4 material from mechanical testing due to better GB and dislocation pinning. Significant casting defects in the form of voids were found though the thickness of the plates from optical microscopy. Optical microscopy revealed these casting defects to be as large as several millimeters in size on rare occasion. Samples tested in this work were visually inspected for the presence of defects at the surface, but it is impossible to discern if pores exist through the thickness before testing.

Tensile testing of the MgSc alloy was performed at a strain rate of 10^{-4} s^{-1} using a Shimadzu 50kN universal testing machine for all three material conditions at room temperature. The samples were cut from two different cast plates, A and B, and manufactured in accordance with ASTM B557M-14 sub-size specimens: cut with a 25mm gauge length, 6mm gauge width, and a thickness of 5mm. The gauge length was tapered to the grips with 6mm radius fillets. Strain was measured by laser extensometer and by digital image correlation (DIC) recorded using a Canon EOS 70D and analyzed using the commercially available VIC 2D software package and the open source nCorr software package. Black spray paint was used to create an optimized random speckle pattern required for DIC analysis.

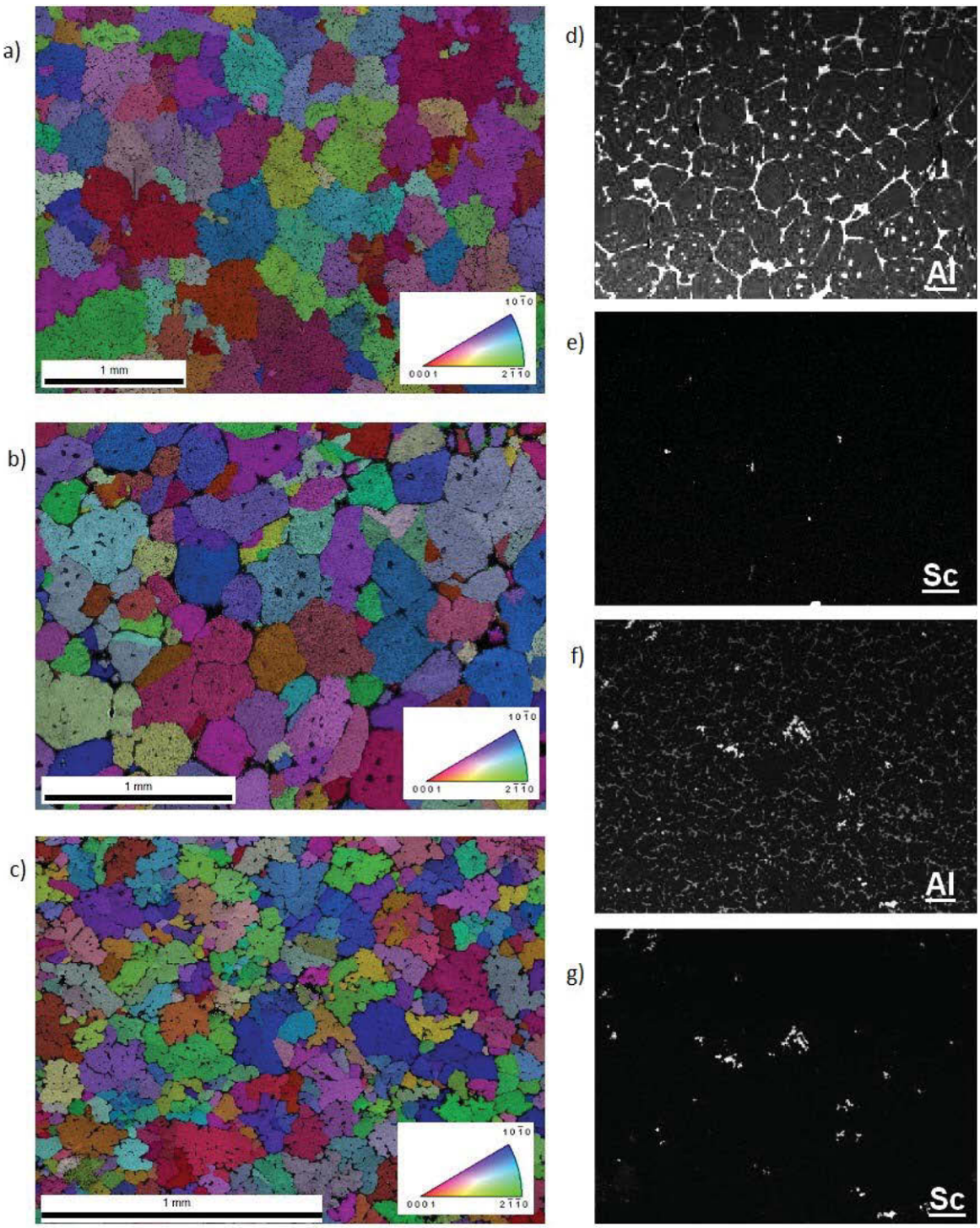

Figure 1. EBSD and EDS characterization of MgSc Microstructure: a) EBSD of the as-cast condition; b) EBSD of the annealed condition; c) EBSD of the T4 condition; d) EDS of aluminum content in the annealed microstructure; e) EDS of scandium content in the annealed microstructure; f) EDS of aluminum content in the T4 microstructure; and g) EDS of scandium content in the T4 microstructure.

Dynamic testing was performed at room temperature in compression and tension on a Split Hopkinson Pressure Bar (SHPB) using 12.7mm and 19.05mm C-350 maraging steel bars, respectively, equipped with strain gauges 914.4mm from the sample-bar interfaces to read the voltage history during testing. Compression samples were constrained by the height of the cast plate and measured 8.7mm in diameter and 5.2mm in length, meeting the design standards of maintaining a diameter to length ratio between 0.5 and 1 as well as maintaining a sample diameter to bar diameter ratio between 0.5 and 1 [12]. The faces of the compression specimens were lubricated to prevent friction from inhibiting strain in the radial direction and ensure that specimens

were only subjected to uniaxial stress [10]. Tensile specimens were designed as dogbone specimens to fit into mechanical grips that thread directly onto the 19.05mm incident and transmission bars. The dogbone specimens contained a gauge length of 10mm with a rectangular gauge cross section of 5mm in height and 3.2mm in depth, tapered with 6mm fillets. A Phantom v710 high speed camera operated at 60,000 frames per second was used to ensure the samples underwent uniform dynamic loading and DIC was attempted for dynamic tensile testing. The strain rates tested were: 700 and 1500 s^{-1} in compression and 800 s^{-1}in tension. Stress-strain relationships were calculated using the standard conversion from incident and transmission bar strain gauge voltage-time histories and may be found in Gray III [12].

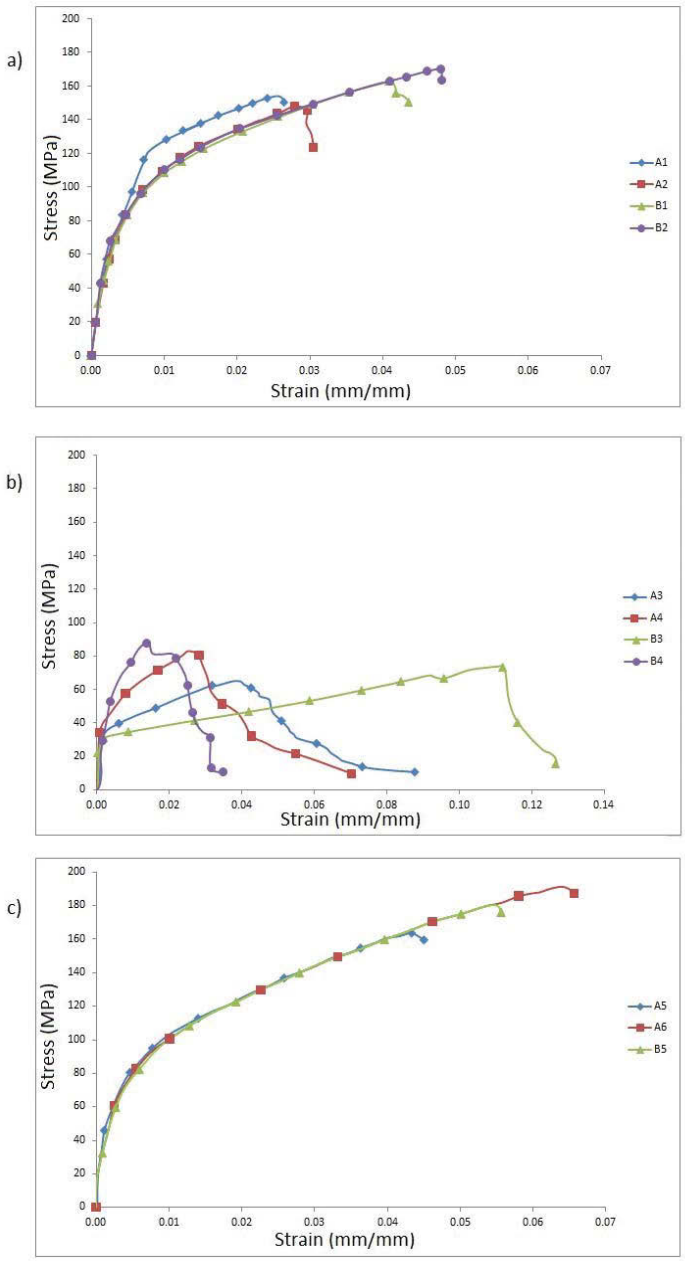

Figure 2. Quasi-static tension results: a) as-cast material; b) annealed material; and c) T4 heat treated material.

Results and Discussion

The stress-strain data obtained from quasi-static tensile tests exhibit a range of responses for the three material conditions, as seen in Fig. 2. The average 0.2% offset yield strength obtained from samples tested from plates A and B was highest in the T4 condition with a value of 61.9 MPa, with average yield strengths of 51.8 MPa and 36.1 MPa for the as-cast and annealed material conditions, respectively. The average ultimate tensile strength (UTS) was also highest in the T4 condition across both plates with a value of 174.8 MPa, with average UTS values of 158.6 MPa and 74.2 MPa for the as-cast and annealed material conditions, respectively. Using the as-cast condition as a reference material, there was a reduction in yield strength and UTS by ~30% and 53%, respectively, for the annealed material, whereas there was an increase in the yield strength and UTS by ~20% and 10%, respectively, for the T4 material.

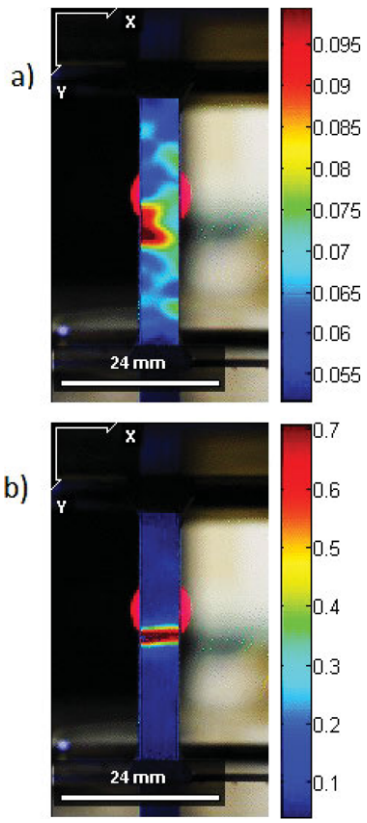

Figure 3. DIC images of quasi-static tension testing: a) immediately before failure; and b) after failure has occurred.

In a general sense the yield strength of the material was found to be closer in comparison to that of pure magnesium (55 MPa) than the yield strength expected from commercial magnesium alloys, such as AZ31 (113 MPa) [6,7]. Additionally, the yield strength and the UTS for similar materials undergoing the same annealing process as samples A3, A4, B3 and B4 have reported to be approximately 216 MPa and 341 MPa, respectively [2]. A significant contributor to the low yield strength values recorded is likely due to the presence of casting defects in the form of voids, which are known contributors to weakening similar materials in tension [8]. In Fig. 2b, the two specimens tested in the

annealed condition from plate B exhibit drastically different stress-strain responses likely caused by local damage initiation, growth, and fracture around interior voids. Digital image correlation analysis showed competing strain regions at multiple points along the gauge length for most the samples tested, from which one such localized strain region became the source of failure, as can be seen by strain maps just before and immediately after failure of sample A6 in Fig. 3. The peak localized strain just before failure in sample A6 was around 0.095, about 70% of the total strain to failure captured by the laser extensometer.

As shown in Fig. 2a and 2c, the as-cast and T4 material conditions exhibit an increase in flow stress throughout the deformation process with failure occurring just after the UTS for all specimens, indicative of strain hardening mechanisms followed by a brittle fracture mode. The average strains to failure for the as-cast and T4 material conditions were 0.038 and 0.056, respectively. Although the annealed material condition had much lower yield strength and UTS, the samples experienced similar, but high in variance, strain hardening as the other material conditions up to similar strains. However, the annealed samples did not fracture immediately after reaching the UTS as the other two material conditions and continued to strain to an average strain failure of ~0.08, ranging from 0.036 to 0.127, indicative of increased ductility.

The explanations for the decrease in yield strength and UTS for the annealed material condition lies primarily with the microstructure along the GBs. As previously stated, an increase in the size of the β-$Mg_{17}Al_{12}$ eutectic phase at the GBs is present in the annealed microstructure, which is the mechanical weak link within the material. The T4 microstructure has a smaller overall grain size, increasing the strength of the material from the well-known Hall-Petch relationship and also resulting in a more even dispersion of smaller regions of β-phase along the GBs. The Mg_5Al_4Sc intermetallic strengthening compounds are also larger in size for the T4 condition, resulting in an increase in GB and dislocation pinning capabilities of the material. These scandium-laden intermetallic compounds are smaller and more dispersed in the annealed microstructure, which does not allow them to properly strengthen the material given the large average size of the β-phase and grains.

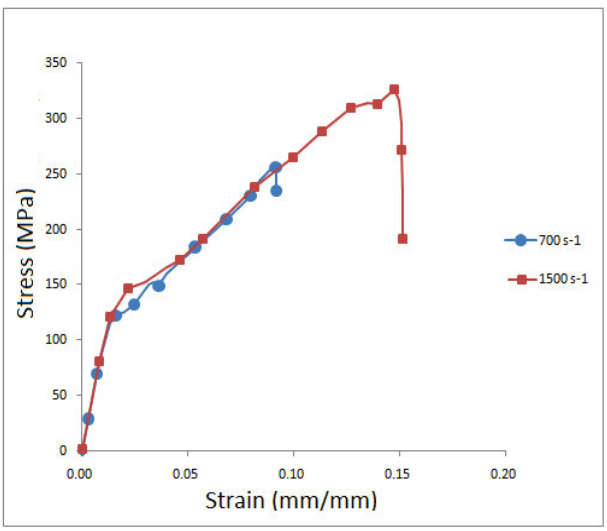

Figure 4. Dynamic compression results for the as-cast material.

Interestingly, there is an increase in ductility in the annealed material, which is hypothesized to be caused by the fracture surface preferring to follow the weak β-phase through the material, resulting in a potentially longer path to fracture indicated by a jagged, inclined fracture surface from visual inspection. A study by Yan et al. [9] showed that a magnesium alloy under low triaxiality constraints of high shear stresses resulted in a ductile fracture surface of increased inclination with the loading direction as compared to high triaxiality constraints leading to brittle fracture perpendicular to the loading direction. Though the apparent embrittlement was due solely to high constraint conditions in [9], there are comparisons to be made with the state of shear stress components and increased ductility from the inclined fracture surfaces in the annealed samples here.

Figure 4 shows the mechanical response of the as-cast material condition in compression at strain rates of 700 s^{-1} and 1500 s^{-1} via SHPB testing. The material exhibits negligible strain rate dependence for the two strain rates tested. A Phantom v710 high speed camera confirmed that the addition of a large mass momentum trap on the incident bar ensured a single deformation pulse imparted on the samples, thus, the drop in stress near the maximum strains shown in Fig. 4 are not material failure, but the samples beginning their free-fall descent away from the pressure bars. The material shows strain hardening up to approximately double that of the estimated yield stress of ~125-150 MPa, which is similar to values known for AZ31 [7] and similar peak stresses obtained from other studies of a similar material [11]. The increase in total strain for the 1500 s^{-1} shot condition is to be expected since there is a larger force imparted on the specimen from an increase in impactor velocity and nearly identical stress pulse duration from the 700 s^{-1} shot. These high strain rate compression tests were able to obtain yield strengths approximately double that of those found from the quasi-static uniaxial tensile testing for the same material condition, providingpromising preliminary evidence for low velocity impact resistance of this alloy.

The mechanical response of the material subject to 700 s^{-1} strain rate tensile SHPB testing indicate poor performance, as the material fractured with negligible gauge length elongation and at a low yield stress. Figure 5a shows the stress-strain response of all three material conditions. Note that it is difficult to impossible to accurately determine the precise Young's modulus and yield stress in SHPB testing, particularly in tension, since the sample does not achieve a uniform state of stress until somewhere after 1-2% plastic strain [12]. It is also important to note that the stress-strain data shown in Figs. 4 and 5 have not undergone any post-processing. The annealed sample is the only one where the yield strength can be somewhat estimated: between 40-70 MPa, which is similar to that material conditions' average quasi-static tensile yield strength of 36.1 MPa.

The samples had an applied speckle pattern for DIC analysis, however, only a few frames exist over the duration of the failure process resulting and was abandoned for the current study. Figures 5b and 5c show the a sample just before and just after fracture, note the lack of elongation in the gauge length. The other specimens exhibited similar fracture processes, but failed more centrally in the gauge section. Two more specimens were tested in tension, but the signal was too weak in the transmission strain gauge to obtain any stress values. It is apparent that the casting defects dominate the fracture mechanics at intermediate strain rate tensile testing as compared to the quasi-static testing. Further studies using casts with limited defects are required to obtain useful high strain rate tensile data.

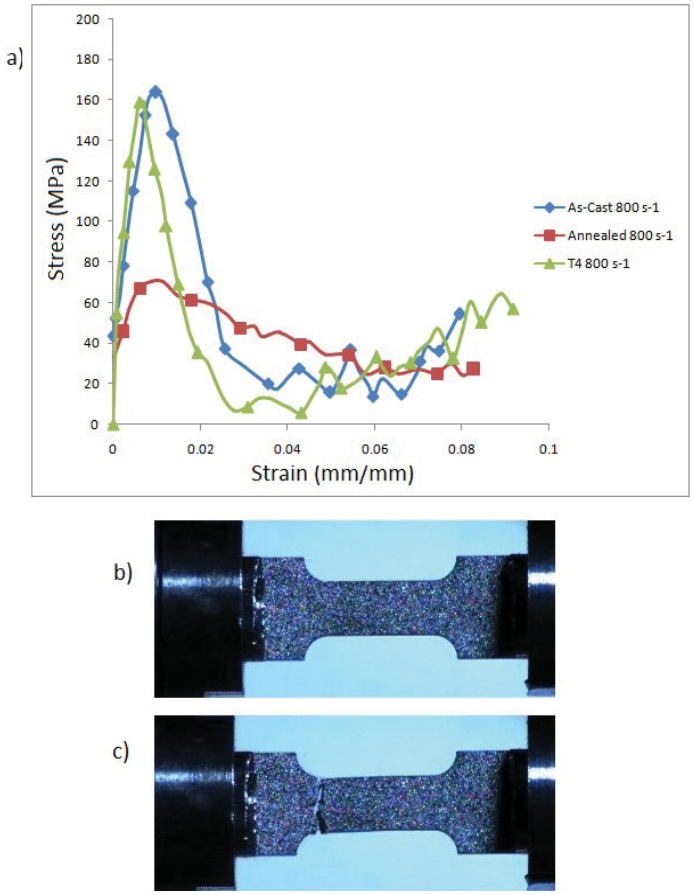

Figure 5. Dynamic SHPB tensile testing: a) stress-strain data for all three material conditions; b) high speed camera footage immediately before failure for the as-cast condition; and c) immediately after failure for the as-cast condition.

Conclusions

Quasi-static and dynamic testing of a cast MgSc alloy of varying microstructures was performed over a range of strain rates from 10^{-4} to 10^{3} in both compression and tension using a conventional universal testing machine and the SHPB technique. Quasi-static tensile tests indicate that the T4 material condition exhibits the most promising mechanical properties due to small β-phase present at the GBs, an increase in the size of scandium intermetallics at the GBs, and a decrease in the average grain size compared to the as-cast and annealed material conditions. Compression testing at two higher strain rates demonstrated an increase in approximate yield stress and more pronounced strain hardening mechanisms over the load duration. Preliminary dynamic tensile testing revealed that the casting defects present in the material dominate the fracture mechanics at intermediate to high strain rates, requiring stock material with fewer defects to properly characterize the material response.Future mechanical testing will be conducted at elevated temperatures for all material conditions and strain rates to gain a broader understanding of the mechanical strengthening potential of scandium in magnesium alloys.

Acknowledgements

This work was partially funded by a UNSW Canberra Rector's Start-Up Grant. The authors would like to acknowledge the technical support and guidance provided by members of the technical service group at UNSW Canberra: Jim Baxter, Patrick Nolan, David Sharp and Thomas Thompson.

References

[1] Mordike, B., & Ebert, T. (2001).Magnesium, Properties – applications – potential. *Materials Science and Engineering.*302 (1), 37-45.

[2] Xiao, D., Song, M., Zhang, F., & He, Y. (2009). Characterization and preparation of Mg-Al-Zn alloys with minor Sc. Journal of Alloys and Compounds. 484 (1), 416-421.

[3] Shalomeev, V., Lysenko, N., Tsivirko, E., Lukinov, V. & Klochikhin, V. (2008). Structure and Properties of Magnesium Alloys with Scandium.Metal Science and Heat Treatment. 50 (1-2), 34-37.

[4] Wang, S., Chou, C., Fann, Y. (2008). Microstructures and mechanical properties of modified AZ31-Zr-Sc alloys. Materials Science and Engineering A. 485 (1), 428-438.

[5] Cizek, L., Greger, M., Pawlica, L., Dobrzanski, L., &Tanski, T. (2004). Study of selected properties of magnesium alloy AZ91 after head treatment and forming. Journal of Materials Processing Technology. 157-158, 466-471.

[6] Diez, M., Kim, H., Serebryany, V., Dobatkin, S., & Estrin, Y. (2014). Improving the mechanical properties of pure magnesium by three-roll planetary milling.*Materials Science & Engineering A.* 612, 287-292.

[7] Dowling, N. (2013). *Mechanical Behavior of Materials.*(4th ed.). (P.65). New Jersey, NJ: Pearson Education.

[8] Weiler, J., Wood, T., Klassen, R., Maire, E., Berkmortel, R. & Wang, G. (2005). Relationship between internal porosity and fracture strength of die-cast magnesium AM60B alloy. Materials Science and Engineering A. 395 (1-2), 315-322.

[9] Yan, C., Ma, W., Burg, V. & Chen, M. (2007). Experiemental and numerical investigation on ductile-brittle fracture transition in a magnesium alloy. Journal of Materials Science. 42 (1), 7702-7707.

[10] Gray, G. (2012). High-Strain-Rate testing of Materials: The Split-Hopkinson Pressure Bar. In Kaufmann, E. (Ed.), *Characterization of Materials.*(2nd ed.). (pp 1-15). New Jersey, NJ: John Wiley & Sons.

[11] Ishikawa, K., Watanabe, H., & Mukai, T. (2005). High strain rate deformation behaviour of an AZ91 magnesium alloy at elevated temperatures.*Materials Letters.*59 (12), 1511-1515.

[12] Gray, G., *ASM HandbooksMechanical Testing and Evaluation*, 2000, vol. 8, pp. 462-476

[13] Ramesh, K., *Springer Handbook of Experimental Solid Mechanics*, 2008

[14] Zhang, J., Guo, Z., Pan, F., Li, Z., & Luo, X. (2007). Effect of composition on the microstructure and mechanical properties of Mg-Zn-Al alloys.*Materials Science and Engineering A.* 456 (1), 43-51.

[15] Von Buch, F., Lietzau, J., Mordike, B., Pisch, A., &Schmid-Fetzer, R. (1999). Development of Mg-Sc-Mn alloys. *Materials Science and Engineering A.* 263 (1), 1-7.